Effect of Nano-fibers on the Stress-Strain Behavior of Semi-Crystalline Poly(ethylene terephthalate) at different Strain Rates

by

Ellann Cohen

SUBMITTED TO THE DEPARTMENT OF MECHANICAL ENGINEERING IN PARTIAL FULFILLMENT OF THE REQUIREMENTS FOR THE DEGREE OF

BACHELOR OF SCIENCE IN MECHANICAL ENGINEERING
AT THE
MASSACHUSETTS INSTITUTE OF TECHNOLOGY

JUNE 2008

Signature of Author:_____
Department of Mechanical Engineering
12/19/2007

Certified by:_____
Mary C. Boyce
Professor of Mechanical Engineering
Thesis Supervisor

Accepted by:_____
John H. Lienhard V
Professor of Mechanical Engineering
Chairman, Undergraduate Thesis Committee

Effect of Nano-fibers on the Stress-Strain Behavior of Semi-Crystalline Poly(ethylene terephthalate) at different Strain Rates

by

Ellann Cohen

Submitted to the Department of Mechanical Engineering
on December 19, 2007 in partial fulfillment of the
requirements for the Degree of Bachelor of Science in
Mechanical Engineering

ABSTRACT

Uniaxial compression tests were performed on amorphous poly(ethylene terephthalate) (PET), amorphous poly(ethylene terephthalate)-glycol (PETG), semi-crystalline PET, and semi-crystalline PET with various amounts of nano-fibers added. The stress-strain behavior for each material at several strain rates is presented. A typical stress-strain curve consists of a relatively steep rise in stress at small strains where the slope is the Young's Modulus. Then, the stress reaches a maximum before decreasing. This stress is called the yield stress. It is the stress at which plastic deformation begins. As the strain continues to increase, the stress begins to rise gradually because of strain hardening. The results show that the initial addition of 1% nano-fibers by weight to semi-crystalline PET increases the yield stress by nearly thirty percent. As the amount of nano-fibers increases, the yield stress remains relatively unchanged. This could be due to aggregation of the nano-fibers at higher weight percent as seen in micrographs. For each material, the yield stress was found to be rate-dependent, scaling with the log of the strain rate at low rates and transitioning to a different rate dependence at high rates. The slope of the yield stress versus ln(strain rate) for each material was approximately parallel. This shows that the addition of nano-fibers does not affect rate sensitivity. The semi-crystalline PETs with nano-fibers did not show any signs of strain hardening up to the strain magnitude tested and needs to be further explored. The maximum stiffness was found to be in the amorphous PET followed by the semi-crystalline PET with 2% by weight nano-fibers blended in. The semi-crystalline PET alone has a much lower stiffness than amorphous PET, but this stiffness increases as nano-fibers are added up until they reach 3% by weight at which the stiffness decreases.

Thesis Supervisor: Mary C. Boyce
Title: Professor of Mechanical Engineering

1. Introduction

Poly(ethylene terephthalate) (PET) is a common thermoplastic material. The most familiar uses today are in plastic bottles, in electrical wire coating, and in packaging. Depending on how the plastic is made, it can take on an amorphous form (clear) or a semi-crystalline form (opaque). The mechanical behavior of these different forms have been studied quite extensively. Dupaix performed uniaxial and plane strain compression tests on amorphous PET and amorphous PETG (poly(ethylene terephthalate)-glycol) over a range of temperatures. It was found that both are similar over the range of strain rates, strain levels, and temperatures tested. [1] Now, we study how the addition of a glycol group to the amorphous PET to form PETG and the addition of different weight fractions of nano-fibers to semi-crystalline PET change their elastic-plastic stress-strain behavior at room temperature at different strain rates.

In this paper, we will report the results from a series of uniaxial compression tests on seven different versions of PET. We will measure and report the stress-strain behaviors for the materials at different strain rates. Tests were performed at low strain rates, 0.0005 s^{-1} to 0.05^{-1}, with a Zwick/Roell Mechanical Tester and at high strain rates, greater than 1000 s^{-1}, with split-Hopkinson pressure bar testing as described in Mulliken and Boyce [3]. The seven versions of PET are amorphous PET, amorphous PETG (poly(ethylene terephthalate)-glycol), semi-crystalline PET, and four semi-crystalline PETs with varying amounts of nano-fibers added.

2. Background

Seven versions of poly(ethyl terephthalate) (PET) were subjected to uniaxial compression testing to obtain their stress strain behavior at room temperature at different strain rates. The two basic versions of PET are amorphous PET and semi-crystalline PET. The amorphous and semi-crystalline PET have the same basic chemical structure, but the amorphous PET is cooled very rapidly preventing any crystals from forming in the material. The amorphous structure results in a transparent material. On the other hand, the semi-crystalline PET is cooled slowly. This allows time for crystallization in the material but not enough time for the entire material to be crystallized rendering a semi-crystalline (part amorphous and part crystalline) structure. Schematics of these two structures can be seen in Figure 1. The crystal and amorphous regions possess different refractive indices and hence render the semi-crystalline PET to be opaque.

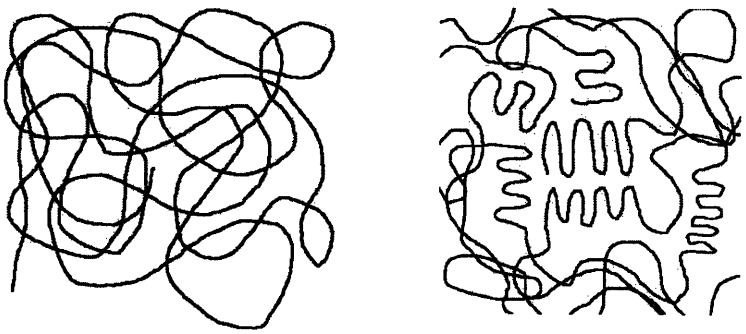

(A) (B)

Figure 1: Pictorial representation of the structure of (A) amorphous PET and (B) semi-crystalline PET

As shown in Figure 2, typical stress strain behavior curves of the elastic-plastic behavior of polymers have several distinct features. The initial slope of the curve is the Young's Modulus, E. The maximum stress reached before the stress drops with increased strain is the Yield Stress, σ_y. After this point, the stress decreases for a certain amount of strain (the strain softening region) and then begins to increase with strain because of strain hardening in the material.

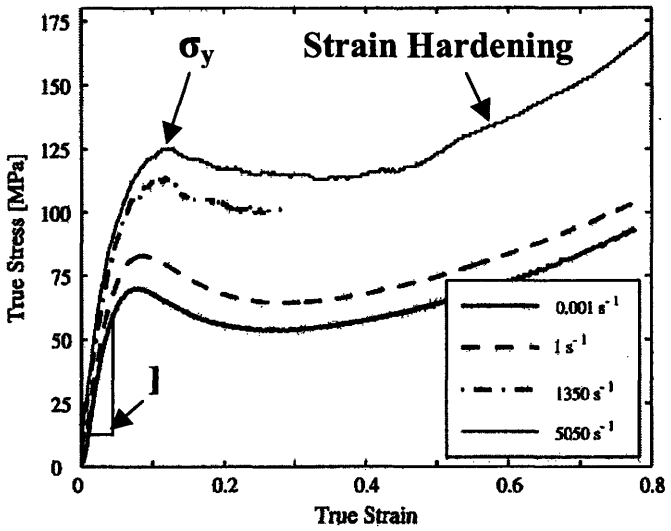

Figure 2: Typical Stress Strain Behavior Curve. This is for polycarbonate at different strain rates from the Mulliken and Boyce paper [1].

Looking at some results of stress strain behavior curves from Dupaix for amorphous PET (Figure 3a uniaxial compression below) and PETG (Figure 3b below) at 25°C, we can see that the typical yield stress for amorphous PET in uniaxial compression at 0.005 s^{-1} is around 70 to 75 MPa and for PETG in compression at 0.01 s^{-1} is around 55 MPa.

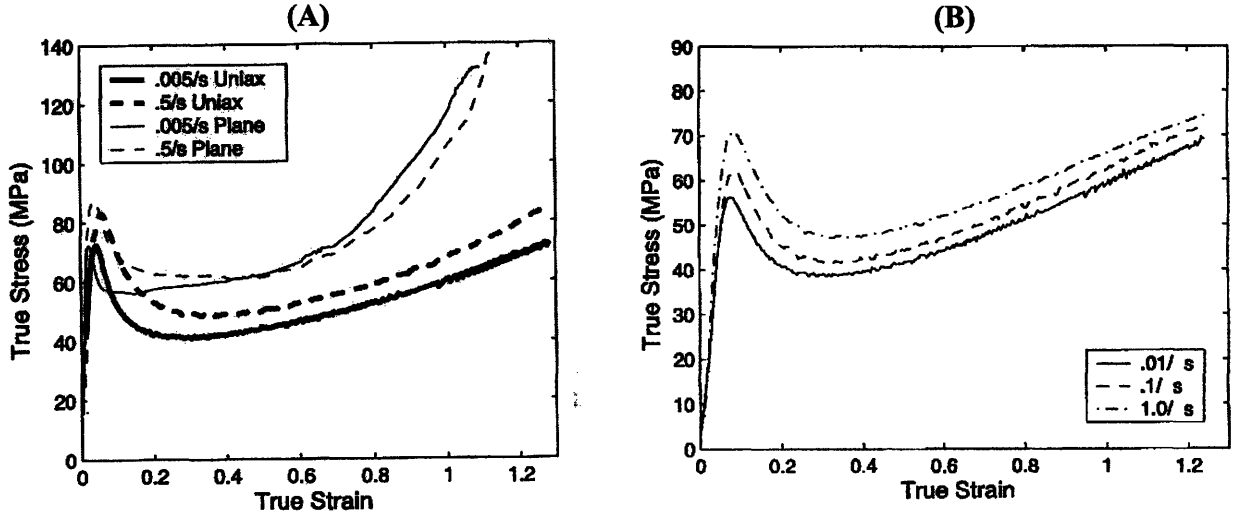

Figure 3: Stress strain behavior curves for (A) amorphous PET and (B) PETG at 25°C from Dupaix [3].

The different types of PET also have a rate dependence. One way of assessing the rate dependence of the elastic behavior is with dynamic mechanical analysis (DMA) testing [1]. It produces a storage modulus curve (shown in Figure 4 below for a PMMA material) as well as a loss modulus curve (not shown). With the DMA data, the beta and alpha transitions regions can be defined. At temperatures greater than the beta transition temperature, local molecular movement freely occurs. An example would be a side group on a molecule can begin vibrating freely or a major group along the backbone of a molecule can rotate. This occurs at lower temperatures than the alpha glass transition region where several large segments along the chain can get involved in the motion. The plot below shows the dependence of the small strain viscoelastic behavior on the strain rate. The storage modulus curve shifts to higher temperatures with increasing strain rate due to time-temperature equivalence of viscoelasticity. In particular, for the PMMA material shown, at room temperature at low strain rates the storage modulus is at 1750 MPA where at high rate, it is at 2250 MPA. At high strain rate the local Beta motion is hindered and provides additional stiffness. For a certain range of strain rates, the storage modulus is fairly constant. Then, if the strain rate is increased by a several order of magnitudes, the storage modulus is much higher.

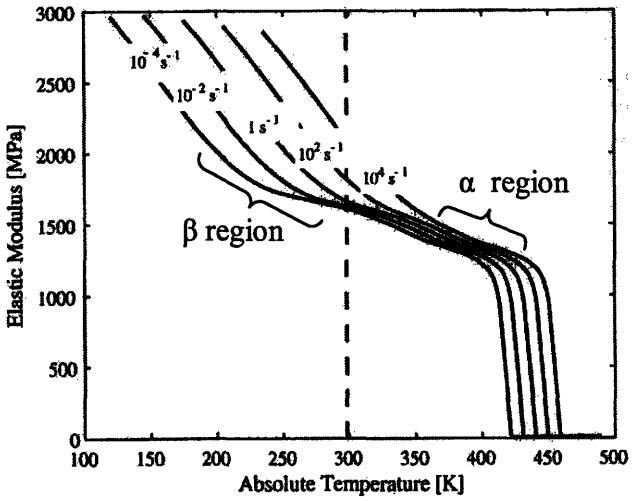

Figure 4: Typical dynamic mechanical analysis (DMA) storage modulus curve for PMMA. The curve shifts with strain rate. [1]

3. Experimental Procedure

3.1 Materials

Tests were performed on amorphous PET, PETG, semi-crystalline PET, and semi-crystalline PET blended with different weight fractions of nano-fibers. The semi-crystalline PET samples were provided by DuPont as tensile coupons (see Figure 5 below). These were then machined into cylindrical shapes with an approximate 2 [mm] thickness and 8 [mm] diameter for the low strain rate tests and a smaller diameter for the high strain rate tests. (See [4] for more information on the high strain rate tests.) The amorphous PET and PETG samples were injection molded into plaques and then cut into the correct specimen shapes and sizes as well. The amorphous PET samples were approximately 7.5 [mm] by 9.5 [mm] by 3.1 [mm] rectangular shapes. The PETG samples were cylindrical with a diameter of 6 [mm] and a thickness of 2.95 [mm].

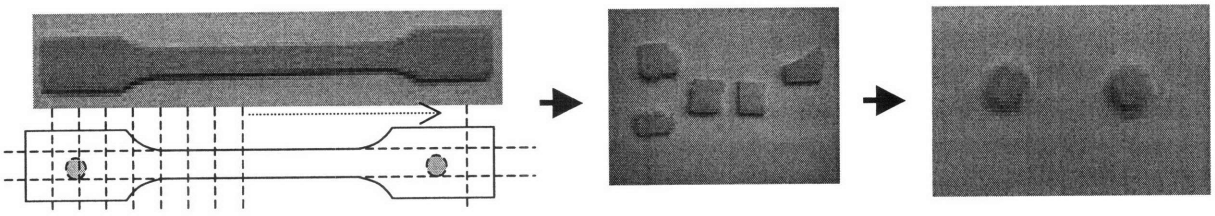

Figure 5: Sample plate from which the semi-crystalline PET samples were cut.

Along with the basic amorphous PET and semi-crystalline PET, the other versions of PET have an additional chemical group along the polymer backbone or are blended with nano-fibers. PETG (poly(ethylene terephthalate)-glycol) is similar to amorphous PET but has additional randomly placed glycol groups along the backbone which disturbs the regularity of the structure preventing any crystallization. The nano-fiber PETs are semi-crystalline PET blended with different weight fractions of nano-fibers. The different semi-crystalline PET samples are provided in Table 1 below.

Semi-crystalline PET sample	Wt % Nano-Fibers	Wt %Wax
PET A	0.0	1.0
PET B	1.0	1.0
PET C	2.0	1.0
PET D	3.0	1.0
PET E	3.0	0.0

Table 1: Semi-crystalline PET samples with weight percent nano-fibers.

The nano-fibers were reasonably well dispersed in the PET, especially at the lowest weight fraction by percent, but there is also significant aggregation of the nano-fibers with increased weight fraction as can be seen in the micrographs in Figure 6 below.

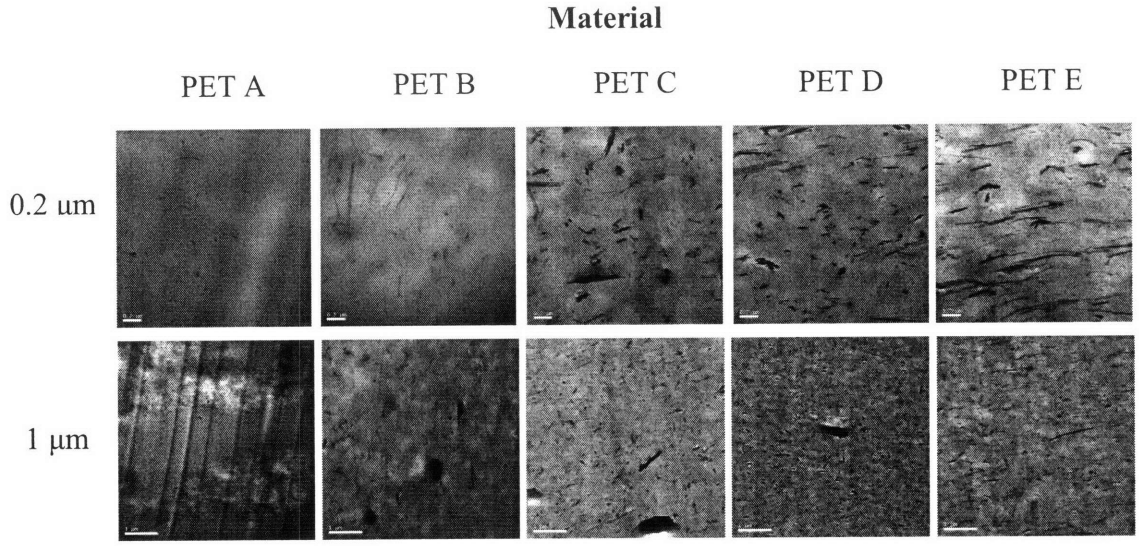

Figure 6: Micrograph of the semi-crystalline PETs (PET A through PET E) at a scale of 0.2 μm and 1 μm, courtesy of M. Weinburg, Dupont.

3.2 Low Strain Rate Tests

For low strain rate testing (strain rates less than 0.1 s^{-1}), the compression tests were performed on a Zwick/Roell Mechanical Tester with a 10kN load cell. For the specimen geometry and material properties, the load cell capacity limited the maximum compression strain to a true strain of -1.0.

For each test, the sample was placed between the two thin films of Teflon and then placed on the compression platens that had been coated with WD40. Both the Teflon and WD40 were used to reduce friction between the sample and the compression platens. Less friction yields a more homogeneous state of strain and stress on the sample and thus a more accurate measure of the uniaxial compression stress versus strain behavior. The data was collected using TestXpert Version 10.0. Tests were conducted at various constant displacement rates, which give the different constant nominal strain rates of 0.0005 s^{-1}, 0.001 s^{-1}, 0.005 s^{-1}, and 0.01 s^{-1} (for our specific tests). It returned the axial force and axial displacement measured during the test. Using the definition of nominal stress, σ_n,

$$\sigma_n = \frac{F}{A_o} \tag{1}$$

where F is the force and A_o is the original cross-sectional area of the sample and the definition of nominal strain, ε_n,

$$\varepsilon_n = \frac{\delta}{l_o} \tag{2}$$

where δ is the displacement of the sample and l_o is the original length of the specimen, the data

was reduced to nominal stress and strain. These quantities were further reduced to true stress, σ, and true strain, ε, using

$$\sigma = \sigma_n(1+\varepsilon_n) \tag{3}$$

$$\varepsilon = \ln(1+\varepsilon_n) \tag{4}$$

The yield stress, σ_y, was found by taking the maximum of the true stress-strain data. Young's modulus, E, was found by determining the slope of a representative curve at low strains. Before each test was run, the specimen and the Teflon were preloaded. This preload value assured full contact with the specimen before beginning the test.

All of the specimens compressed very homogeneously. Two examples of specimens before and after compression (PETG and PET B) are shown below in Figure 7.

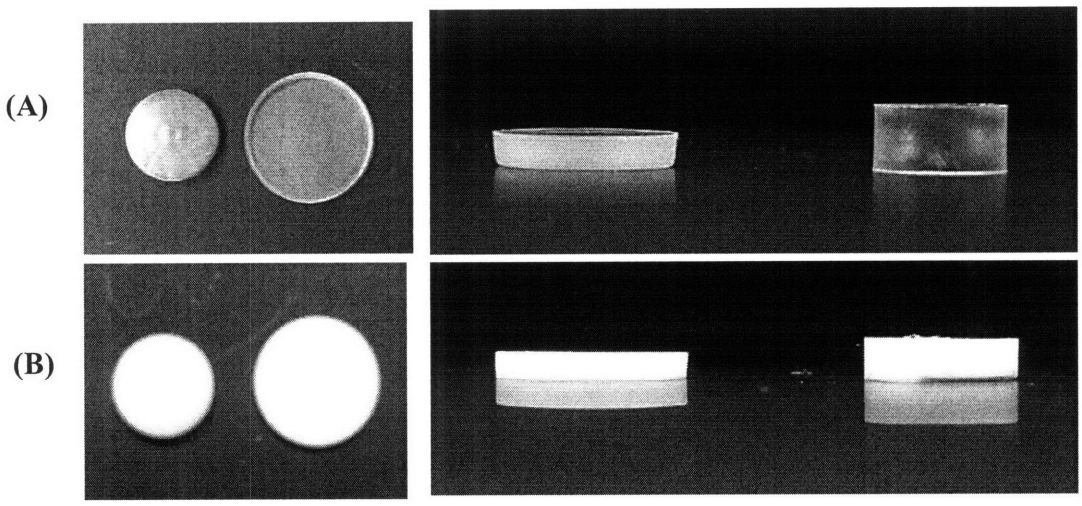

Figure 7: PETG (A) and PET B (B) samples before and after compression

3.3 High Strain Rate Tests

High strain rate tests were performed on a Split Hopkinson bar apparatus following the procedure described in Mulliken and Boyce [1]. The data reported here were obtained by MIT mechanical engineering undergraduate Joshua Garvin (personal contact) during his UROP project.

4. Results and Discussion

After performing the various compression tests and analyzing the data using the equations given in Section 3, the true stress versus true strain curves for each material at four different strain rates, 0.01 s^{-1}, 0.005 s^{-1}, 0.001 s^{-1}, and 0.0005 s^{-1} were found. Tests were conducted to the largest strain possible for each material as governed by the maximum allowable load of the load cell (allowing a strain of about 0.6 for amorphous PET, and around 1.1 for PETG and all the semi-crystalline PETs). The results are shown below in Figures 8 through 14. A typical curve consists of a sharp rise in stress in the beginning. The slope of this rise is

Young's Modulus. Then, the stress reaches a peak and then drops. The peak is called the yield stress. This is where the material begins to plastically deform. As the strain continues to increase, the stress will increase slightly. This increase at the higher strains in called strain hardening. In general, the yield stress of each material increased with an increase in strain rate. The result for the yield stress for amorphous PET and PETG match fairly closely to the results obtained by Dupaix (Figure 4). For Dupaix's amorphous PET at a strain rate of the 0.005 s^{-1}, the yield stress was approximately 70 MPa. The same is true for the results below. For Dupaix's PETG results, the yield stress was around 55 MPa for a strain rate of 0.01 s^{-1} and the same result was found below. This confirmed the validity and repeatability of our testing procedure.

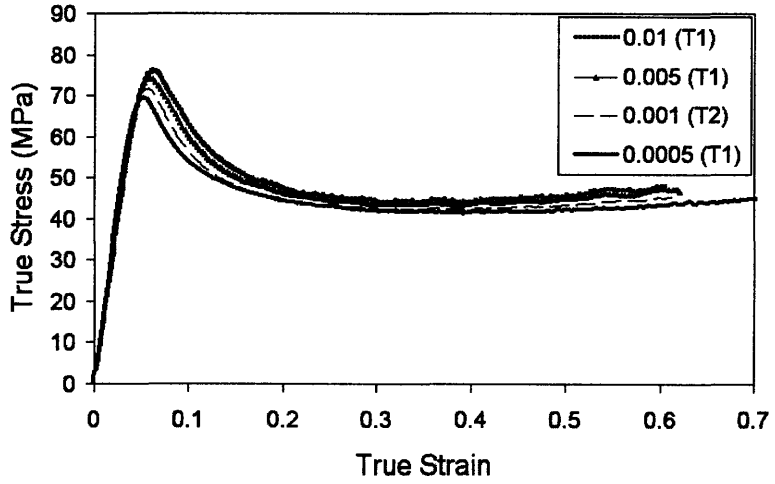

Figure 8: Stress-strain curve for amorphous PET at different strain rates (s^{-1}).

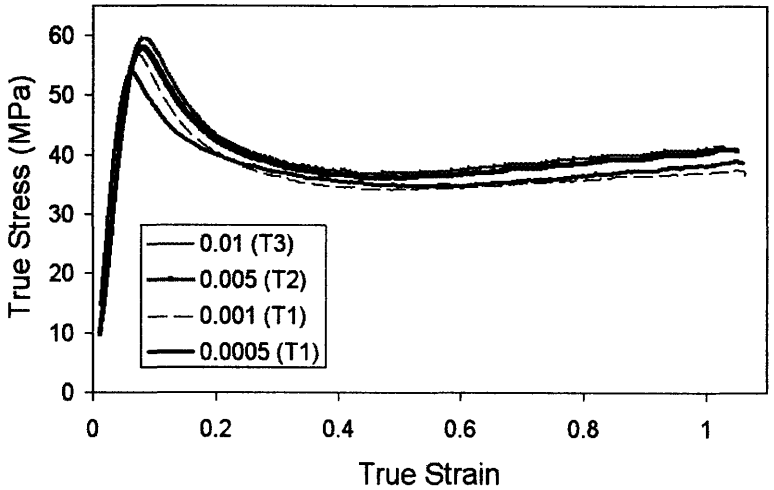

Figure 9: Stress-strain curve for PETG at different strain rates (s^{-1}).

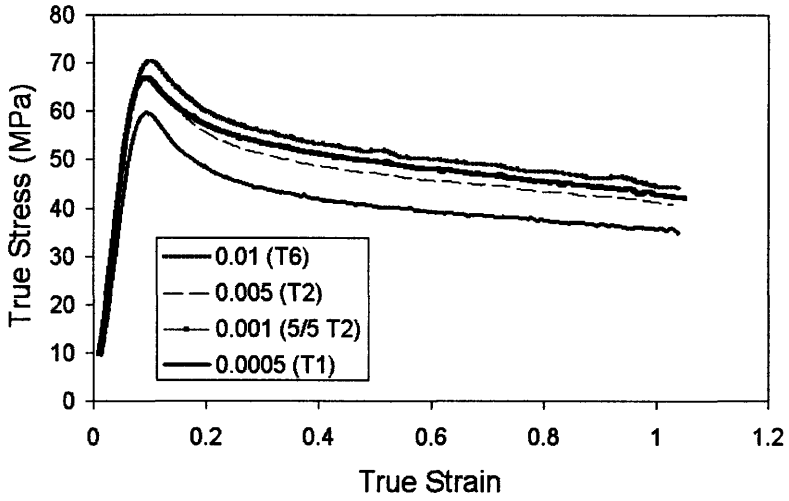

Figure 10: Stress-strain curve for PET A at different strain rates (s^{-1}).

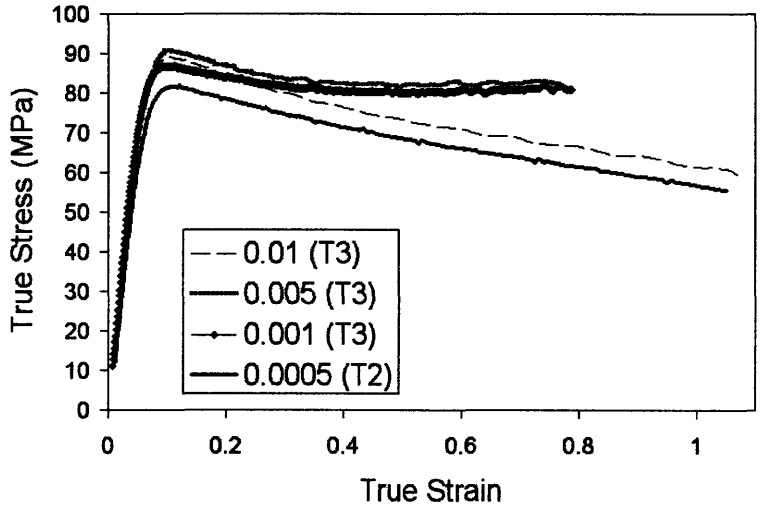

Figure 11: Stress-strain curve for PET B at different strain rates (s^{-1}).

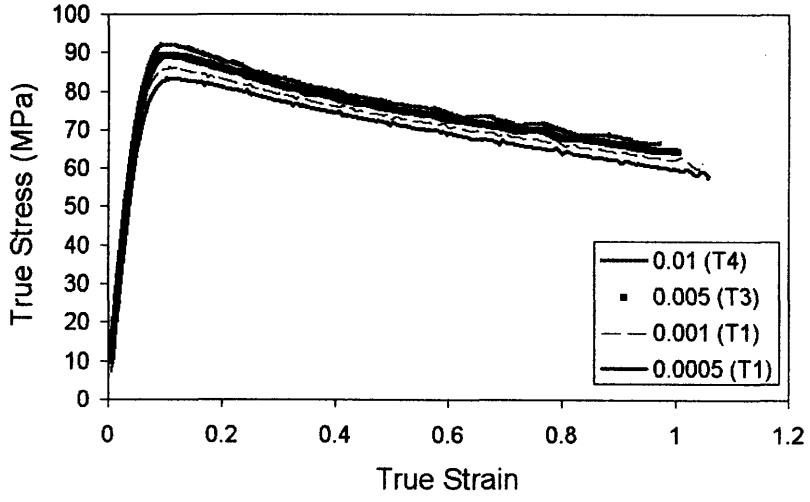

Figure 12: Stress-strain curve for PET C at different strain rates (s^{-1}).

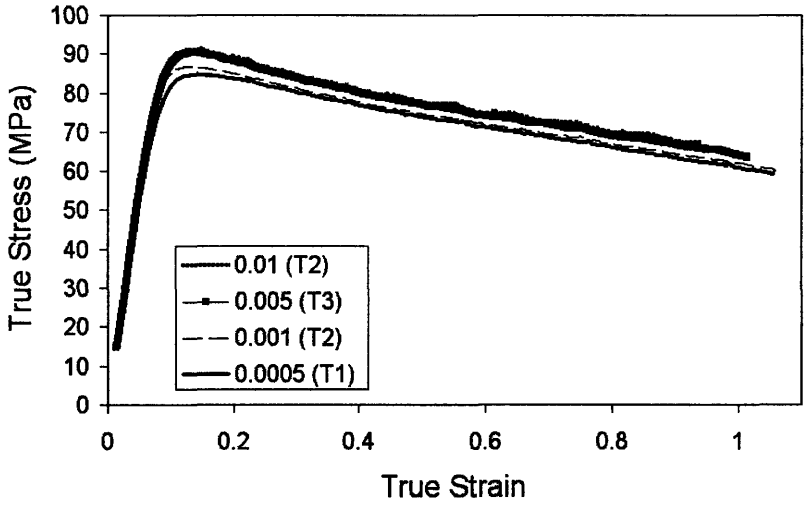

Figure 13: Stress-strain curve for PET D at different strain rates (s^{-1}).

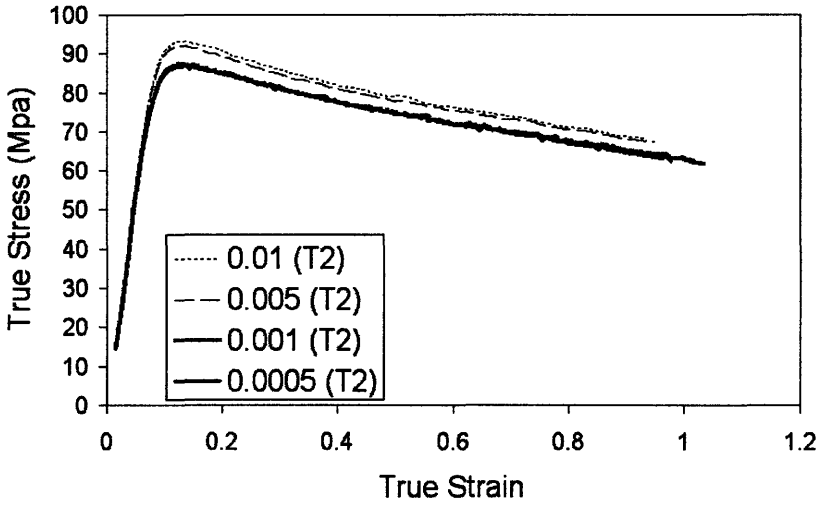

Figure 14: Stress-strain curve for PET E at different strain rates (s^{-1}).

We also looked at the correlation between the yield stress and the natural log of the strain rate. The results are below in Figure 15. In general, there was a defined linear correlation between the yield stress and the natural log of the strain rate. Each material except PET B had excellent correlation.

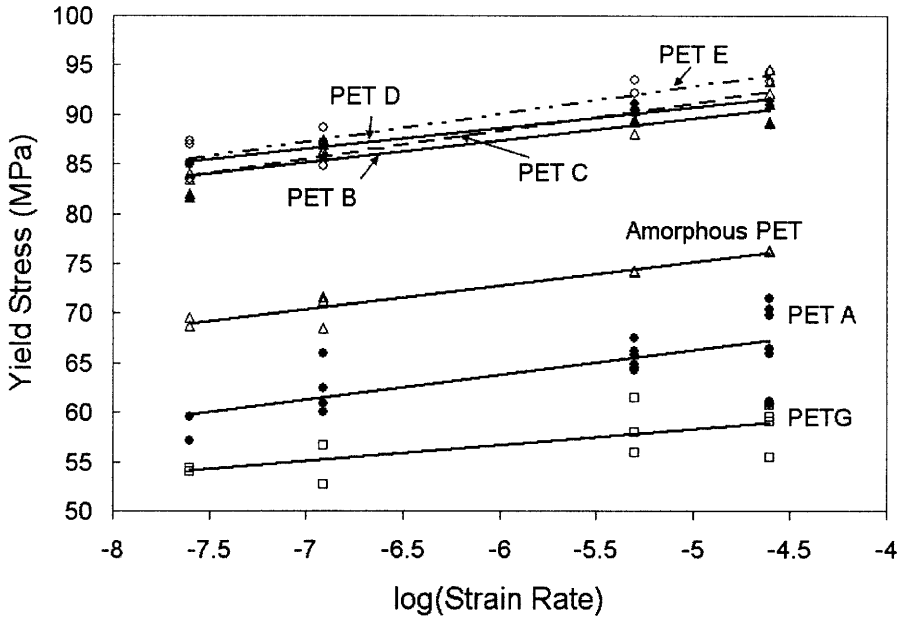

Figure 15: Yield stress versus the natural log of the low strain rates for all PET materials.

Looking at the overall trend (Figure 15), the slopes for each material are approximately the same. This means that the addition of nano-fibers has not affected the rate sensitivity of the materials. The yield stress increases because the nano-fibers are carrying some of the load when load is transferred to the fibers through local shearing of the matrix via the shear lag local transfer mechanism. A schematic of one fiber centrally located in a piece of material is shown below in Figure 15. The PET matrix material that is in direct contact with the fiber is constrained to remain in contact with the fiber; therefore it undergoes local shear straining at the fiber/matrix interface which transfers stress to the fiber via a shear lag load transfer mechanism. [4]

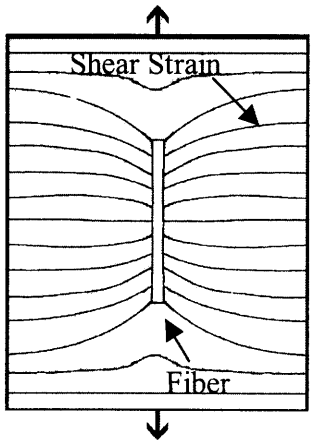

Figure 16: Shear strain surrounding a fiber in a material that is under uniaxial tension.

The Eyring model [5] of rate dependent plasticity was also examined. This model predicts the rate dependence of the yield stress. The Eyring model is

$$\dot{\varepsilon} = \dot{\varepsilon}_o \exp(-\frac{\Delta G - \sigma \cdot \Omega}{K \cdot \theta}) \tag{5}$$

where $\dot{\varepsilon}$ is the strain rate, ΔG is the energy barrier to the event, σ is the stress, Ω is the activation volume, K is the Boltzmann constant, and θ is the absolute temperature in Kelvin. Since we are examing only one temperature, we simplify the equation and set

$$\dot{\alpha}_o = \dot{\varepsilon}_o \exp\left(-\frac{\Delta G}{k\theta}\right). \tag{6}$$

By inserting equation (6) into equation (5), only two unknowns are left, $\dot{\alpha}_o$ and Ω. Rearranging the solution, it can take on slope intercept form matching the curves in Figure 15 with

$$\sigma = \frac{K\theta}{\Omega}\ln\dot{\varepsilon} - \frac{K\theta}{\Omega}\ln\dot{\alpha}_o \tag{7}$$

The resulting values for $\dot{\alpha}_o$ and Ω are in Table 2 below.

	Ω (10^-21) [m^3]	$\dot{\alpha}_o$ [s^{-1}]
AmPET	1.72	1.12E-16
PETG	2.48	2.68E-18
PET A	1.63	2.09E-14
PET B	1.84	1.76E-20
PET C	1.44	7.41E-17
PET D	1.94	1.11E-21
PET E	1.45	3.00E-17

Table 2: Eyring model constants for each material.

Tests were also performed at high strain rates by Joshua Garvin. His results are below (Figure 17). The ending strain of each of tests depends on the pressure used in the Hopkinson bar set-up to achieve different strain rates and do not reflect any failure of the specimen. These specimens were also found to deform in a homogeneous manner. The trends are similar to the trends at low strain rates. Typically, the higher the strain rate, the higher the yield stress.

(A)

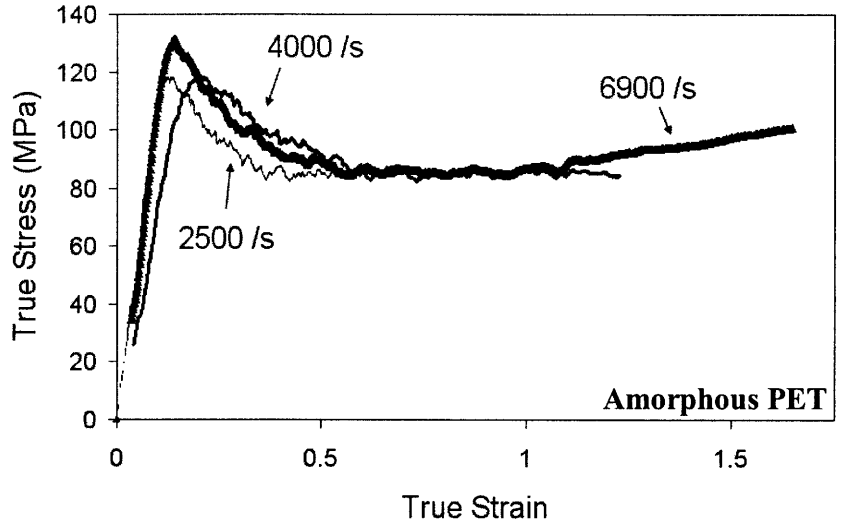
4000 /s
6900 /s
2500 /s
Amorphous PET
True Stress (MPa)
True Strain
0
20
40
60
80
100
120
140
0
0.5
1
1.5

(B)

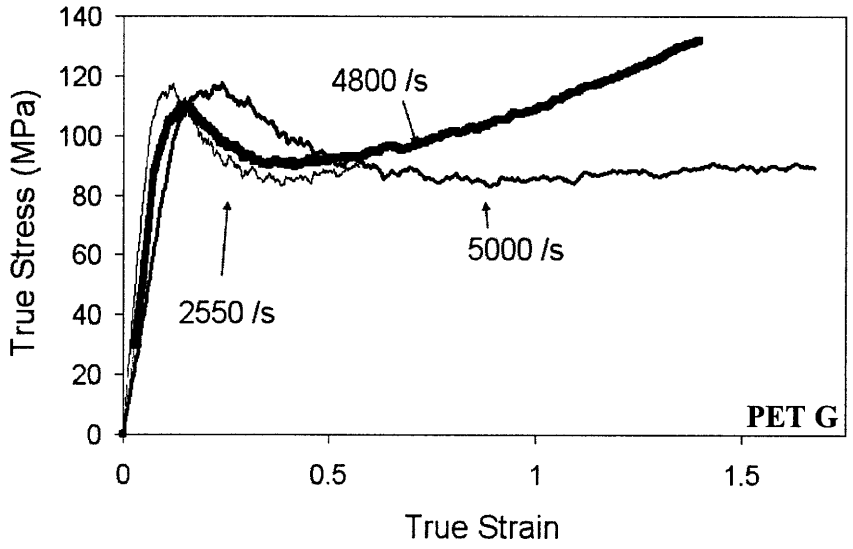
4800 /s
5000 /s
2550 /s
PET G
True Stress (MPa)
True Strain
0
20
40
60
80
100
120
140
0
0.5
1
1.5

(C)

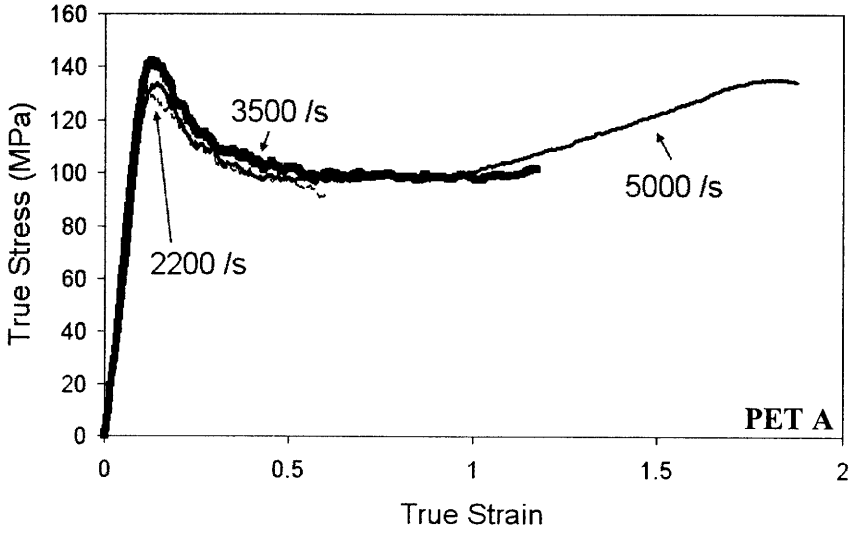
3500 /s
5000 /s
2200 /s
PET A
True Stress (MPa)
True Strain
0
20
40
60
80
100
120
140
160
0
0.5
1
1.5
2

(D)

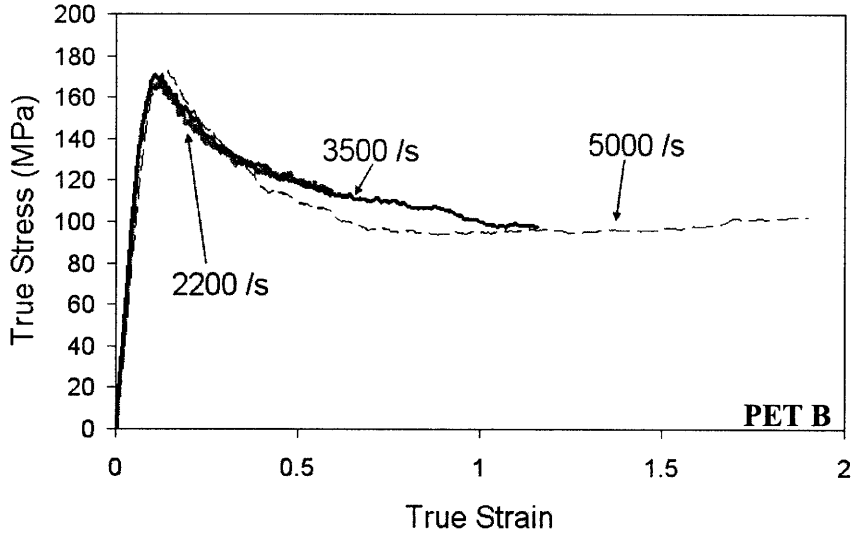
True Stress (MPa)
True Strain
3500 /s
5000 /s
2200 /s
PET B

(E)

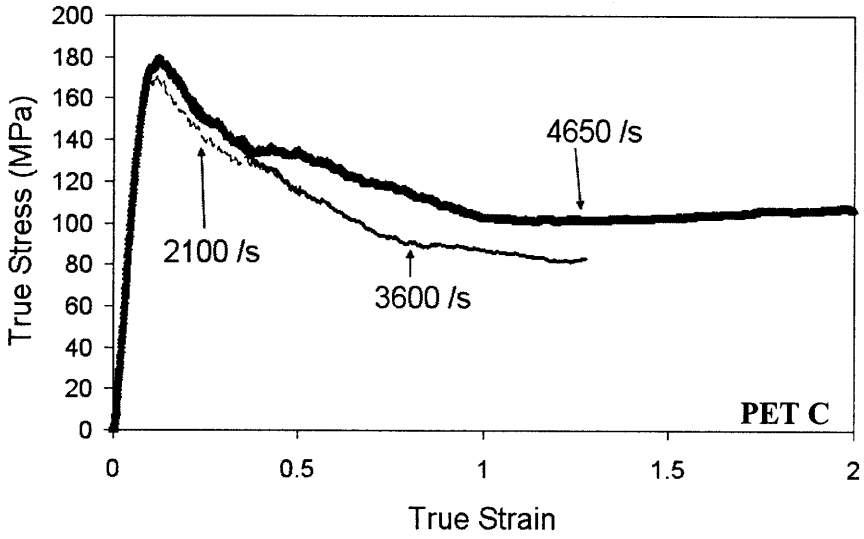
True Stress (MPa)
True Strain
4650 /s
2100 /s
3600 /s
PET C

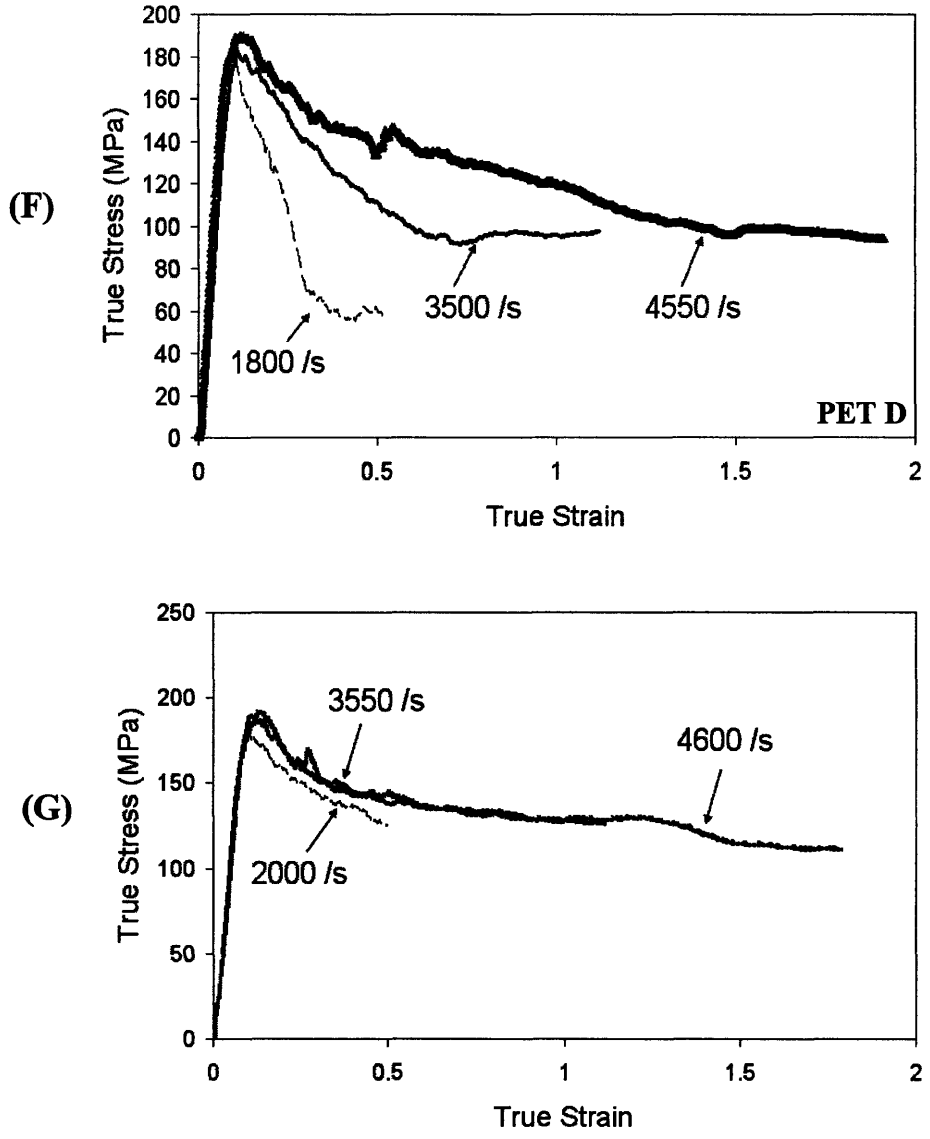

Figure 17: Stress Strain curves for each material, (A) Amorphous PET (B) PETG (C) PET A (D) PET B (E) PET C (F) PET D (G) PET E, at different high strain

The yield stress versus natural log of the strain rate curves for these much higher strain rates yields a much higher slope (Figure 18 below). Extrapolation of the low rates Eyring curve is seen to predict much lower yield stresses at the very high rates than actually found in the experiments. This indicates a much stronger rate dependence of the yield at the very high rates.

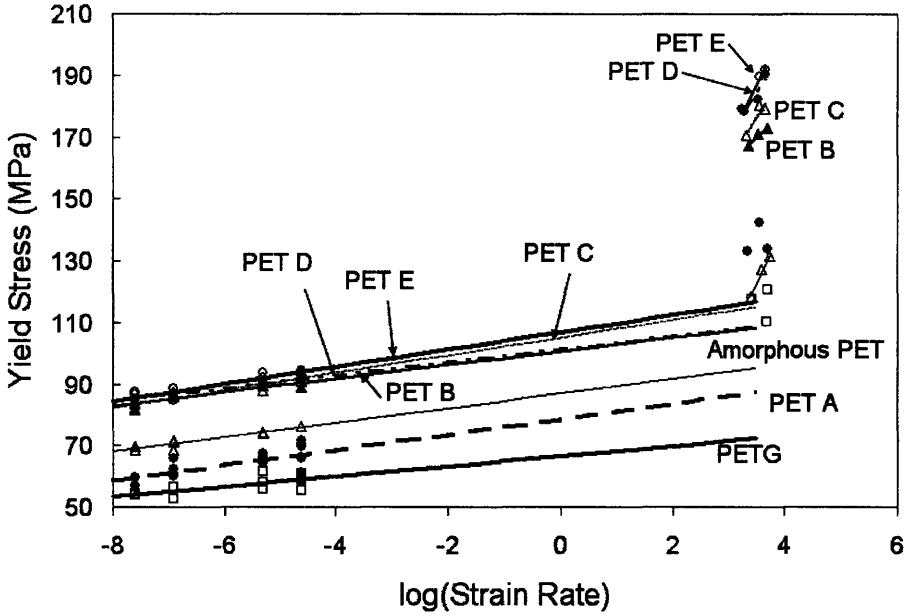

Figure 18: Yield stress vs. log(strain rate) for all materials and strain rates.

This difference in slope can be accounted for if you look at Dynamic Mechanical Analysis (DMA) data (Figure 19). This DMA data was collected by Sai Sarva (personal contact). DMA shows the relationship between strain rate and the storage modulus. For a certain range of strain rates (at one temperature), the storage modulus is fairly constant corresponding to the lower rate dependence of yield observed for the low strain rates in Figure 19. Then, if the strain rate is increased by a several order of magnitudes, the storage modulus is much higher since the Beta transition region has shifted and Beta motions are now hindered at the high rates and any variation will change the modulus much more. This increased stiffness observed at higher strain rates corresponds to the increased rate sensitivity of the of the yield stress observed at the very high rates.

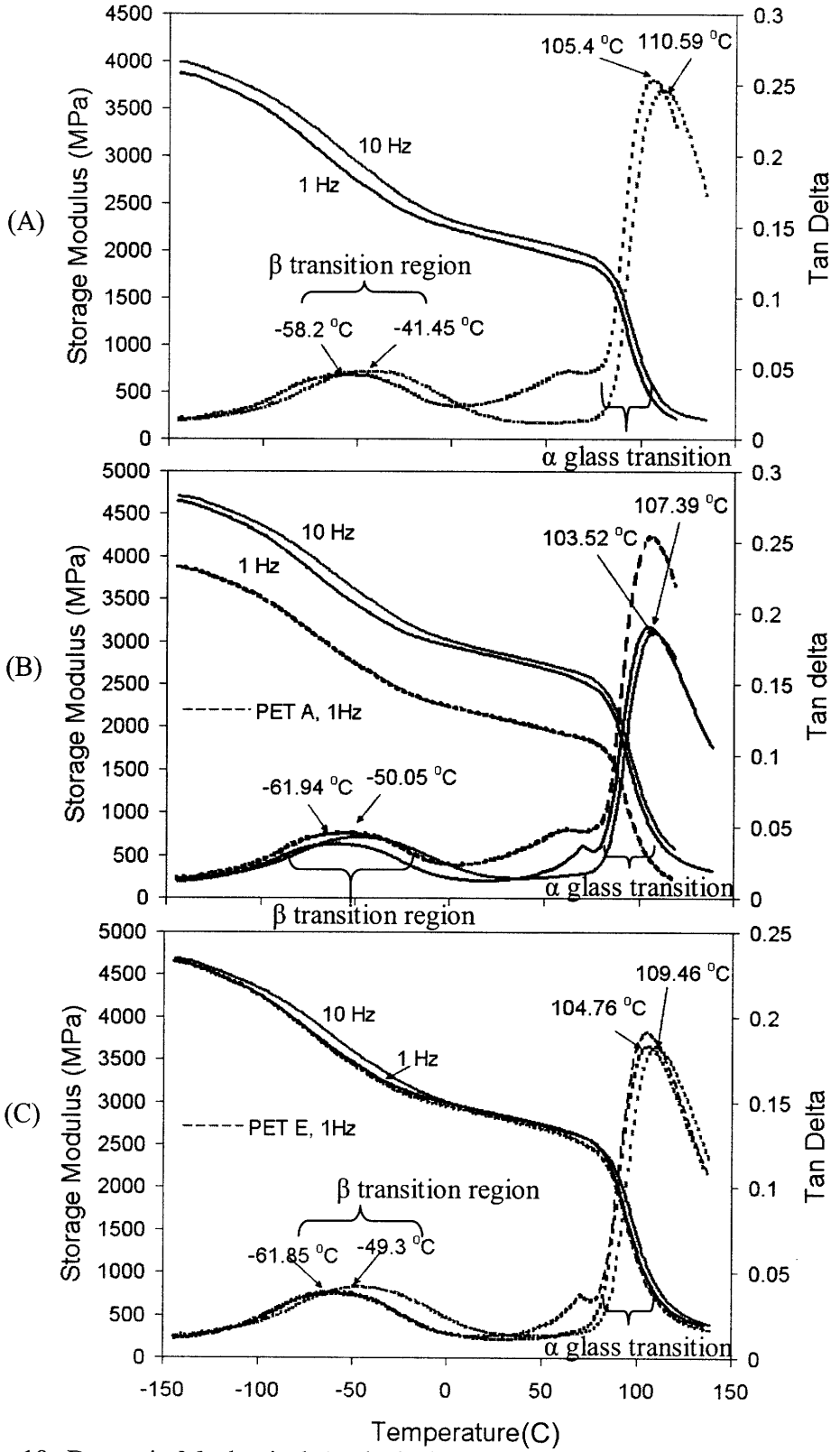

Figure 19: Dynamic Mechanical Analysis (DMA) results for PET A (A), PET E (B), and PET D (C) at two different rates.

The next comparison is a plot comparing the stress versus strain curves of each material at each of the tested strain rates. This is plotted for each of the low strain rates (Figure 20). At each strain rate, the stress-strain curves for each material are similar compared to the other materials. The results at 0.01 s^{-1} and 0.0005 s^{-1} strain rates are the clearest. PETG always has the lowest yield stress followed by the homogeneous semi-crystalline PET, the amorphous PET and then the nano-filled semi-crystalline PETs. In general, the nano-filled semi-crystalline PETs followed a pattern of PET B, PET C, PET B, and PET A for increasing yield stress, but they all had very similar yield stresses, so they overlapped a few times as seen in (B) and (C) in Figure 19.

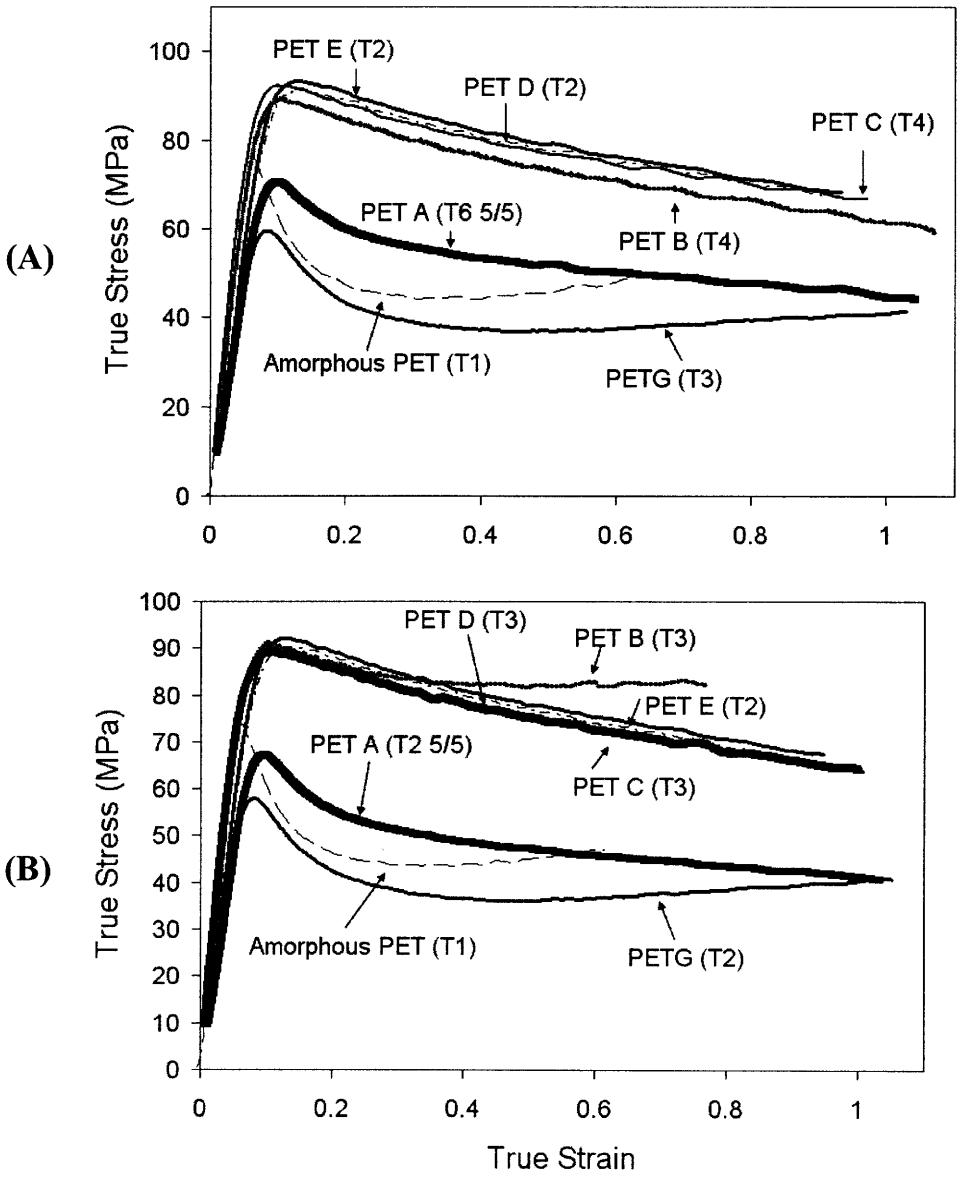

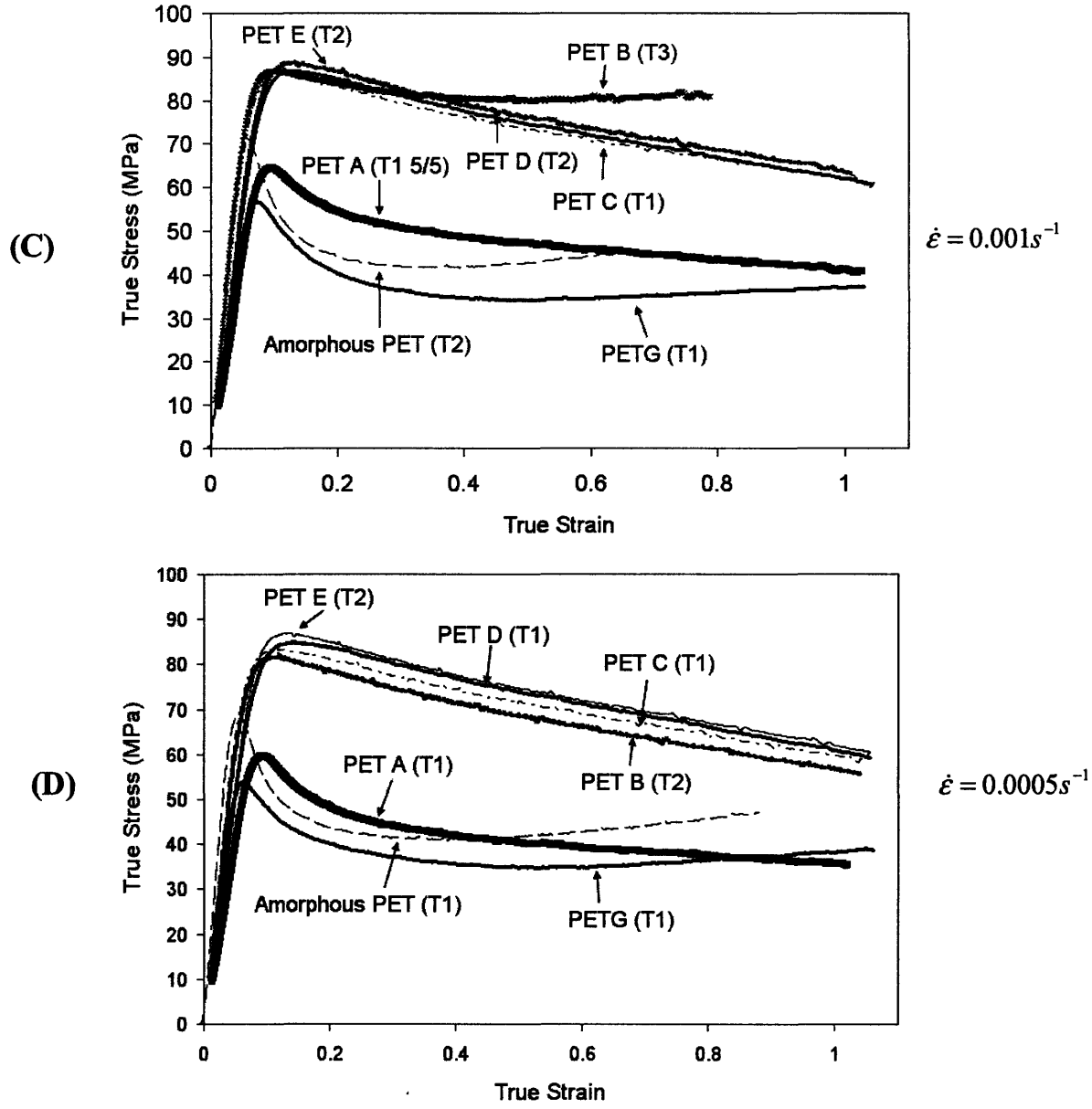

Figure 20: Stress Strain curves for each material at different strain rates (A) 0.01 s^{-1} (B) 0.005 s^{-1} (C) 0.001 s^{-1} (D) 0.0005 s^{-1}

The homogeneous semi-crystalline and nano-filled semi-crystalline PETs had an unusual behavior at the higher strains of each strain rate. Instead of experiencing strain hardening as with most materials (the amorphous PET and PETG are examples), they each continued to have a negative stress-strain slope till the end of the test. A few times, the PET B experienced strain hardening, but in general the materials did not show any signs of strain hardening. This could be due to the fact that the maximum strain tested was limited by the load cell. At higher strains, the materials might still exhibit a strain hardening behavior. Each of these materials stress-strain behavior curves also have the same shape prior to yielding. The amorphous PET and the PETG

behave normally as their stresses drop immediate after they reach their yield stresses, but some higher strain later their stress begin to rise again.

Figure 21 examines yield stress as a function of the weight fraction of the nano-fiber filler. The addition of only one percent weight nano-fibers makes an incredible difference in the yield stress of the material, nearly 30 percent. The addition of more nano-fibers does not continue to increase the yield stress. This can be explained by shear lag. The schematic in Figure 21 (A) represents one fiber (like a nano-fiber) centered in a material. As the material in put under stress, the material surrounding the fiber experiences shear strain, thus transferring load to the fiber. If fibers are clumped together like in Figure 21 (B), the material only transfers shear stress to the fibers with which it is in direct contact. This leaves the interior fibers stress free (i.e. not carrying any load) and prevents them from strengthening the material. [4]

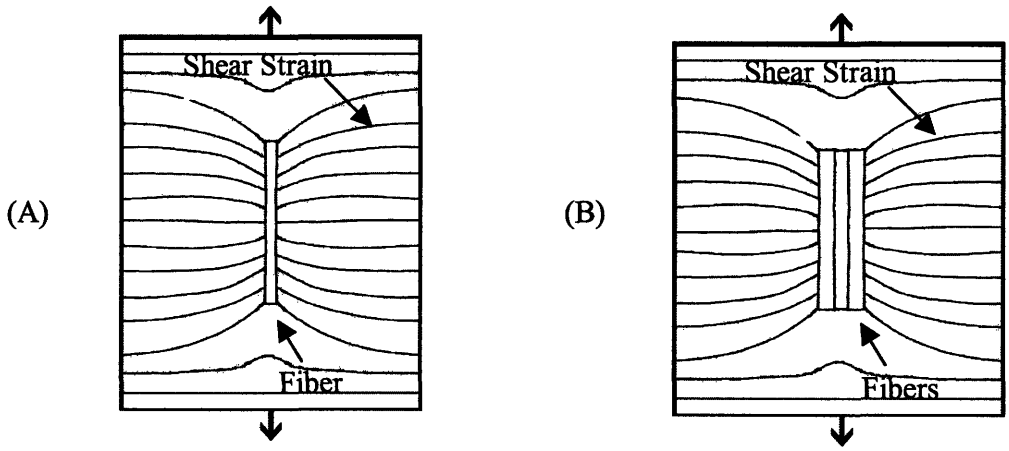

Figure 20: Shear lag schematic showing the difference shear strains in the material surrounding one fiber (A) and surrounded multiple clumped fibers (B). This is the difference in shear strains in well dispersed versus aggregate situations.

At the lowest percent weight, the nano-fibers are well dispersed in the PET. This causes a nice increase in the ability of the material to withstand stress (compared to no nano-fibers). Then, as more nano-fibers are added, the nano-fibers tend to clump together (as can been seen in the micrographs in Figure 2.) This reduces the effect of adding more because the material only sees one clump instead of several nano-fibers. In the future, we would do more tests on a material with nano-fibers only being 0.5 percent weight to see where this jump in yield stress occurs. Also, we could treat the nano-fiber surfaces to better disperse the nano-fibers in the PET.

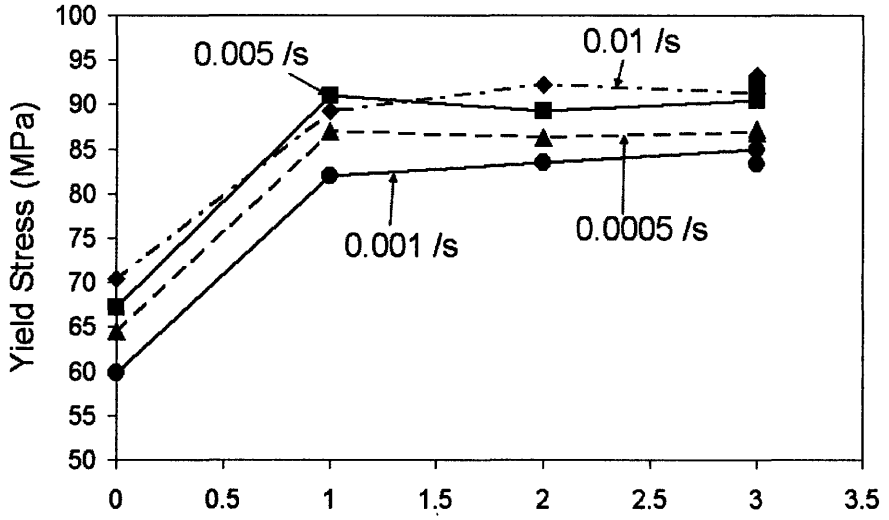

Figure 21: Yield stress versus percent weight of nano-fibers in material

The results comparing the Young's Modulus of nano-fiber filled semi-crystalline PETs to each other by the percent weight of the nano-fibers in the material can be seen in Figure 22 below. In general, the peak Young's Modulus occurs when the nano-fibers are 2% weight of the PET for the low strain rates, but then it drops when reaching 3% weight. For the higher strain rates, the Young's Modulus continues to increase with each addition of nano-fibers, but the biggest increase is still from 0% to 1% weight. This can also be explained with the same argument as used to describe Figure 21, shear lag.

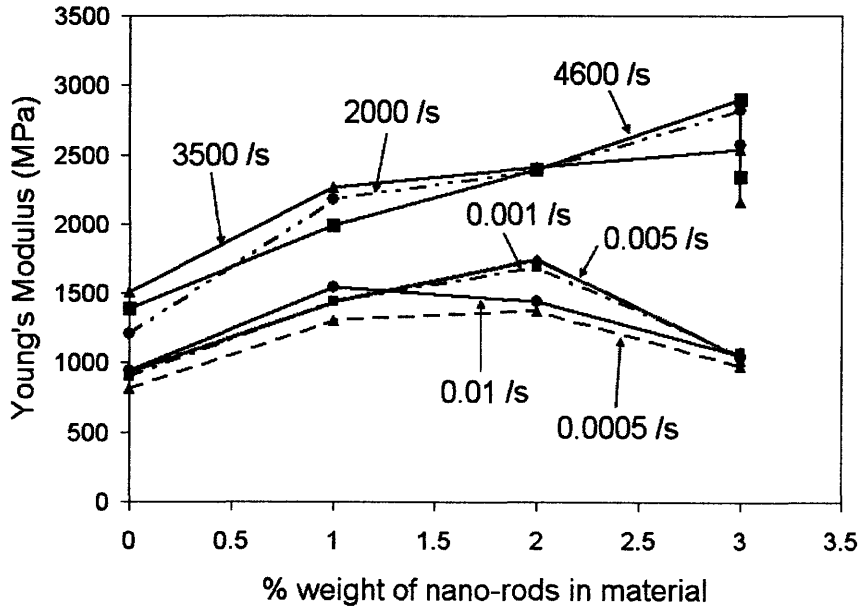

Figure 22: Young's modulus (MPA) versus percent weight of nano-fibers in material

Repeatability results for the low strain rate tests are shown in the appendix in Figures 22 – 28. PET A had the least repeatable results. This could have been caused by several different things. First, it could have been due to where the samples were cut out of the bar in Figure 6. This location may have caused preferential alignment in the crystals. A way to correct this would be to heat the samples after they are cut and anneal them. Any of these could have caused the repeatability to be less exact.

The low strain rate compression tests yield very clean results. The samples come out perfectly nearly every time. Pictures of the results before and after compression can be seen in the appendix in Figures 29 – 35.

All results for the yield stress and Young's modulus are in Table 3 in the appendix. For each material at each strain rate, the middle or most average curve was chosen to represent the tests at the strain rate. The yield stress and young's modulus for that representative test is displayed. Also, each of the curves chosen to represent its rate and material is listed in this table.

Acknowledgments

I gratefully acknowledge conversations with Prof. Mary Boyce and Renaud Rinaldi helping with testing, analysis, and understanding materials better. Also, I thank Josh Garvin and Sai Sarva for letting me use some of the data they collected.

References

[1] Dupaix, R.; Boyce, M. C. *Polymer.* 2005; 46: 4827-38.

[2] Dupaix, R.; Boyce, M. C. *Mechanics of Materials.* 2007; 39: 39-52.

[3] Mulliken, A. D.; Boyce, M. C. *Int. J. Solids Struct.* 2006; 43: 1331-56.

[4] Courtney, Thomas. Mechanical Behavior of Materials. 2nd Edition. McGraw Hill. Boston, 2000.

[5] Eyring, Henry. *Journal of Chemical Physics.* 1936; 4: 283-291.

Appendix

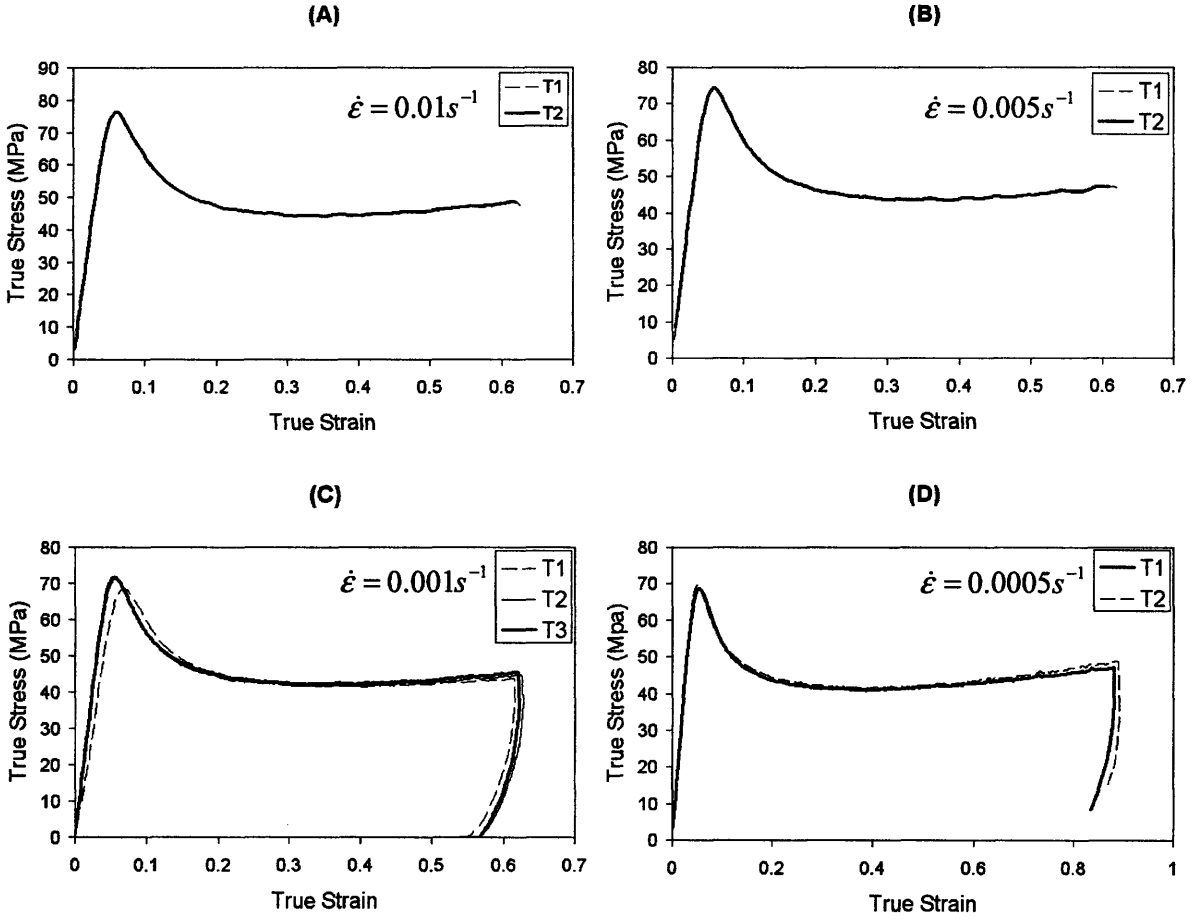

Figure 23: Stress Strain results for Amorphous PET at different Strain Rates (A) 0.01 s^{-1} (B) 0.005 s^{-1} (C) 0.001 s^{-1} (D) 0.0005 s^{-1}

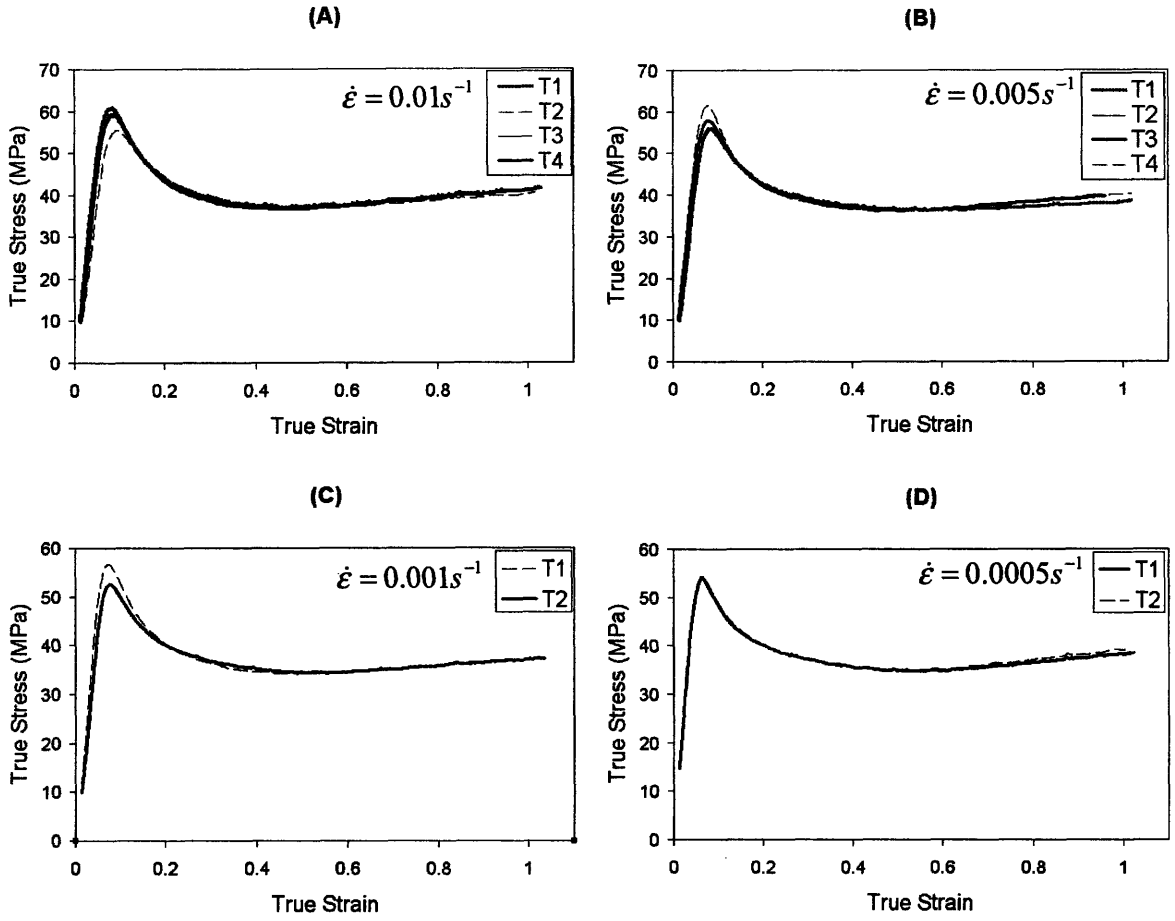

Figure 24: Stress Strain results for PETG at different strain rates (A) 0.01 s^{-1} (B) 0.005 s^{-1} (C) 0.001 s^{-1} (D) 0.0005 s^{-1}

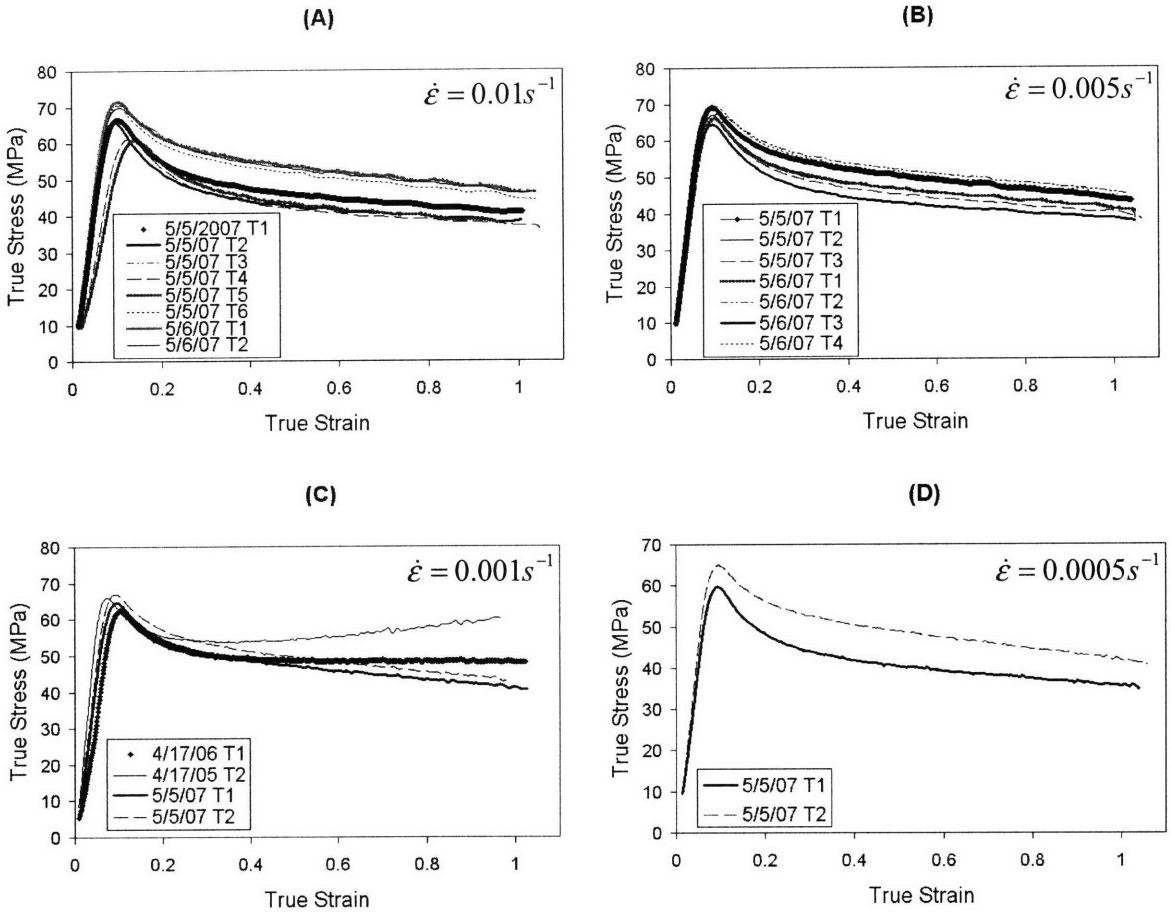

Figure 25: Stress Strain results for PET A at different strain rates (A) 0.01 s^{-1} (B) 0.005 s^{-1} (C) 0.001 s^{-1} (D) 0.0005 s^{-1}

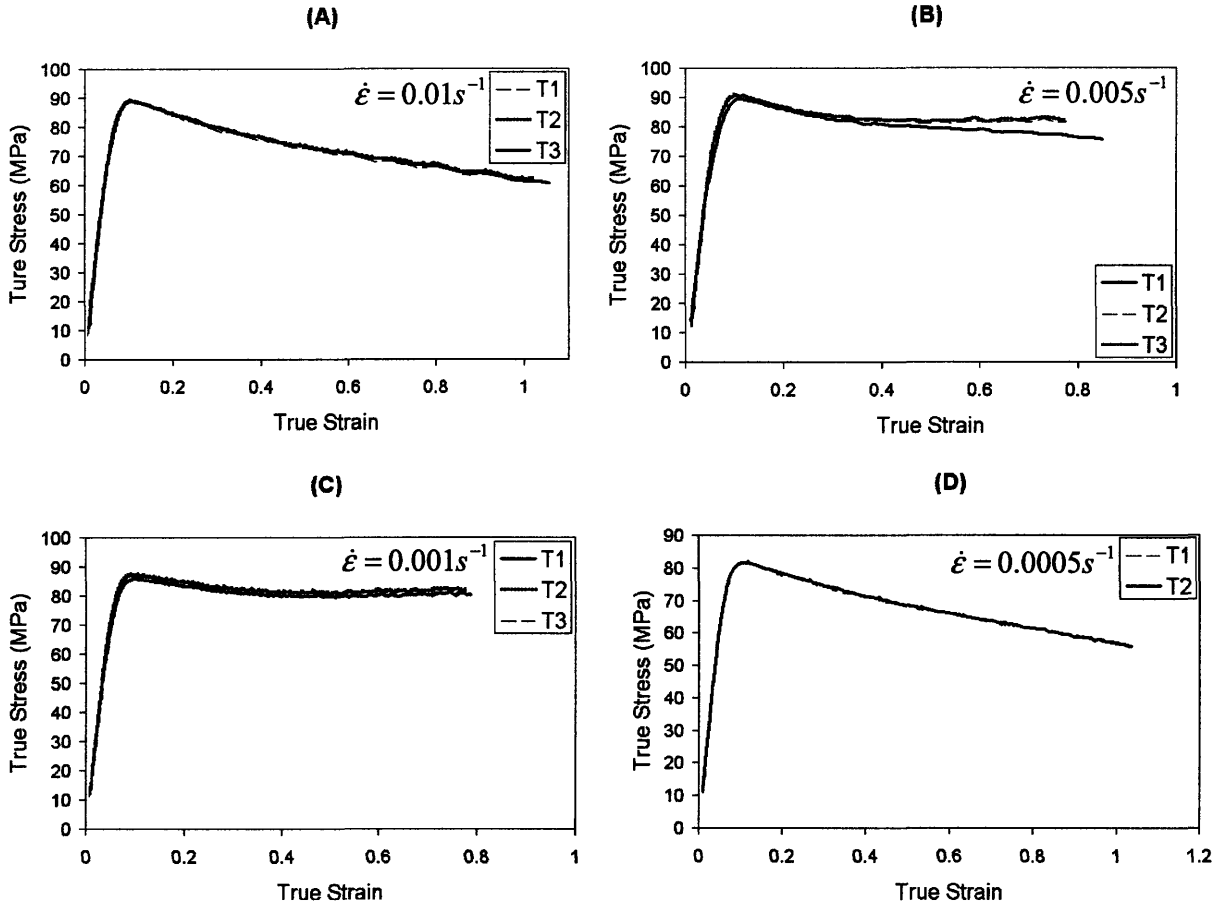

Figure 26: Stress Strain results for PET B at different Strain Rates (A) 0.01 s^{-1} (B) 0.005 s^{-1} (C) 0.001 s^{-1} (D) 0.0005 s^{-1}

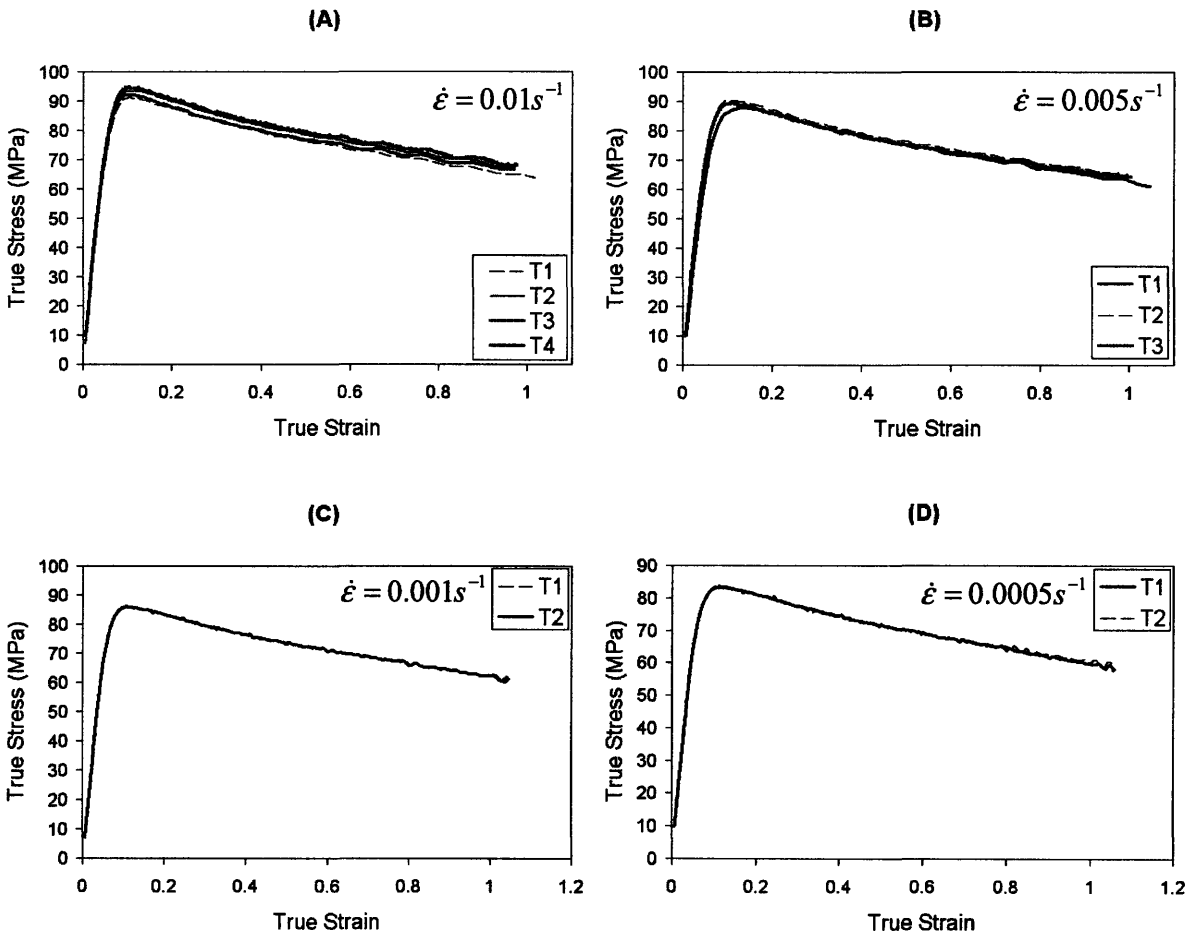

Figure 27: Stress Strain results for PET C at different strain rates (A) 0.01 s^{-1} (B) 0.005 s^{-1} (C) 0.001 s^{-1} (D) 0.0005 s^{-1}

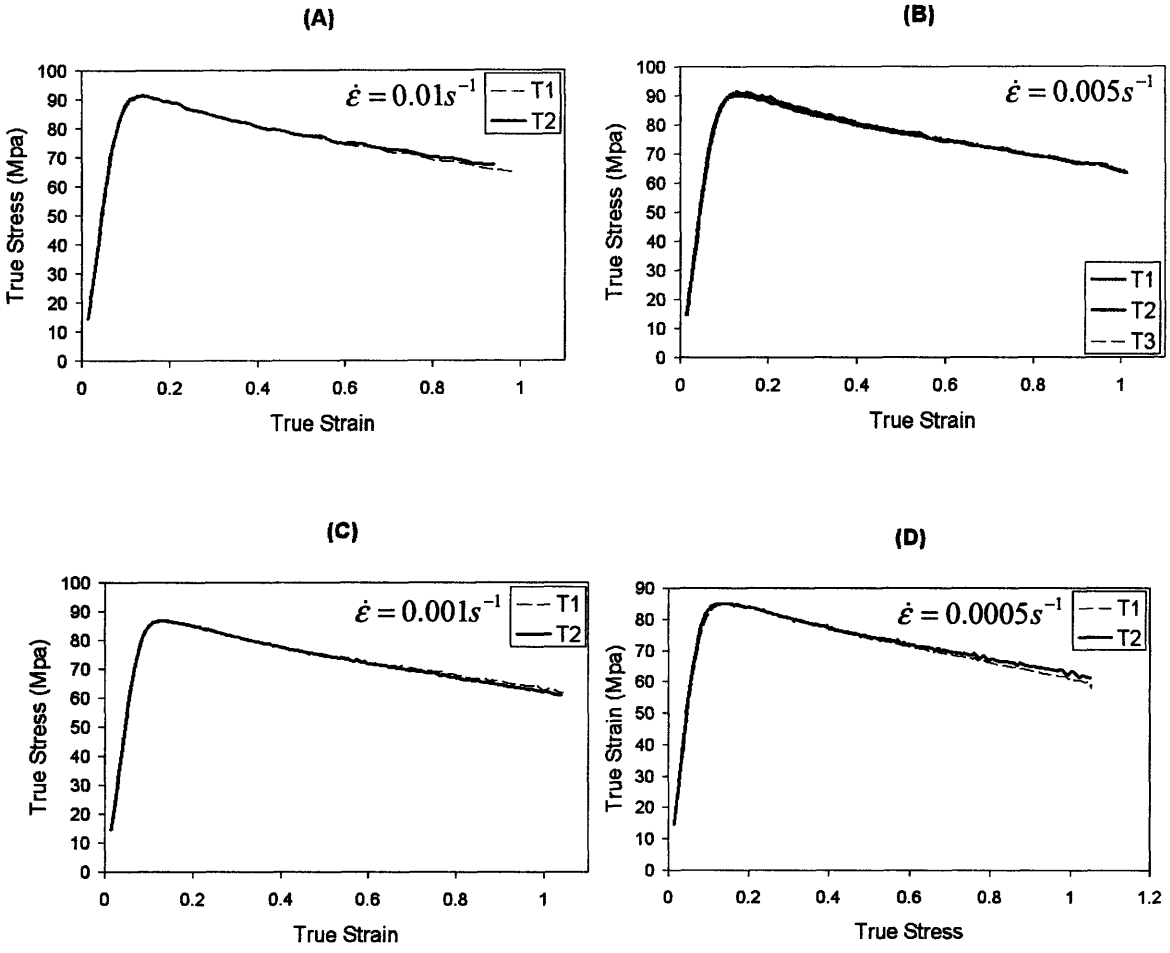

Figure 28: Stress Strain results for PET D at different strain rates (A) 0.01 s^{-1} (B) 0.005 s^{-1} (C) 0.001 s^{-1} (D) 0.0005 s^{-1}

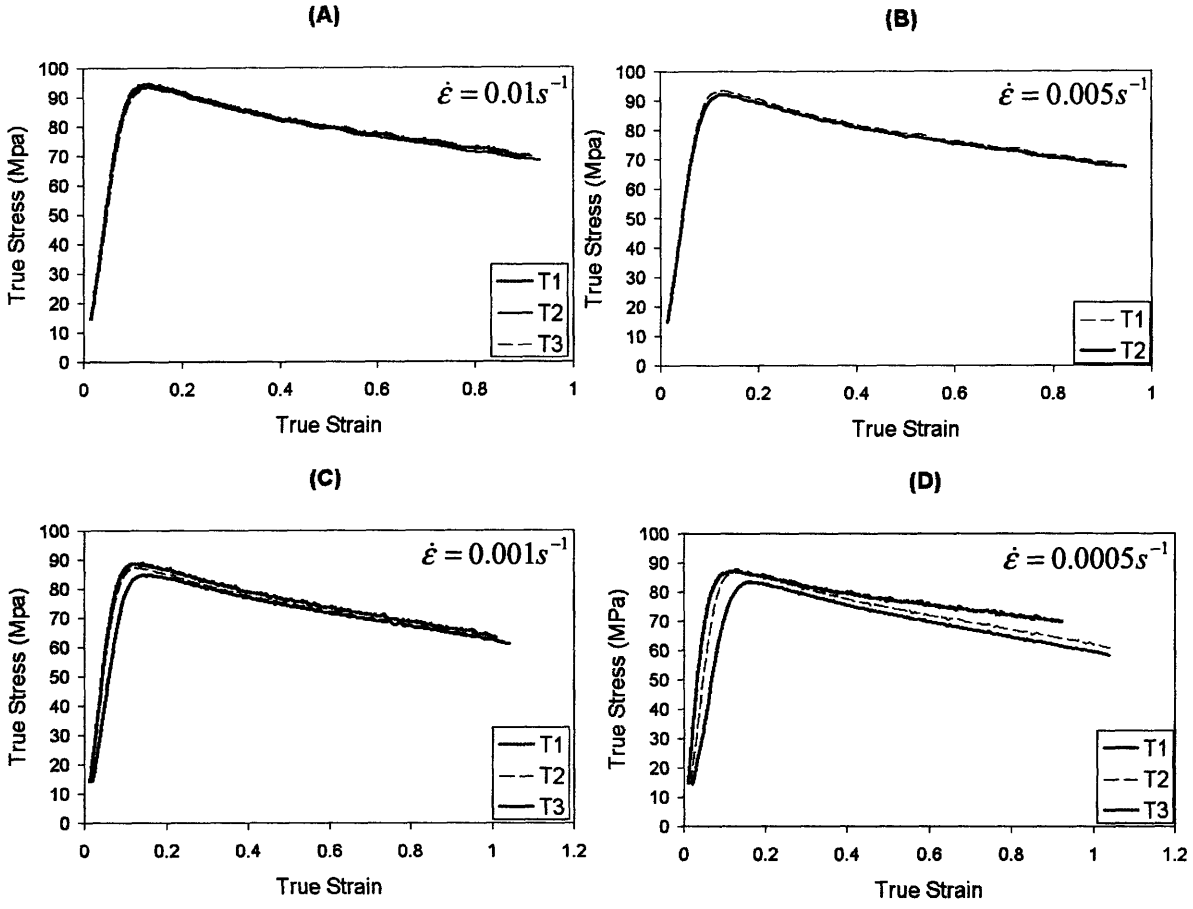

Figure 29: Stress Strain results for PET E at different strain rates (A) 0.01 s^{-1} (B) 0.005 s^{-1} (C) 0.001 s^{-1} (D) 0.0005 s^{-1}

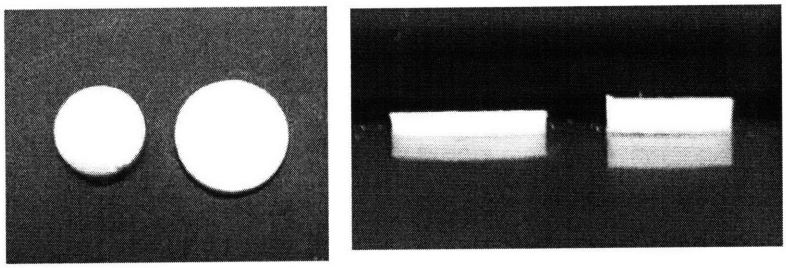

Figure 30: PET E samples before and after compression

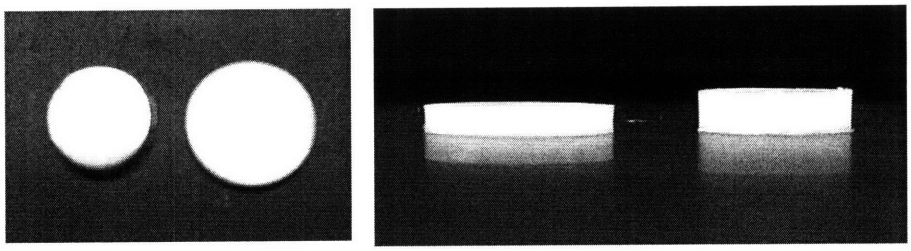

Figure 31: PET D samples before and after compression

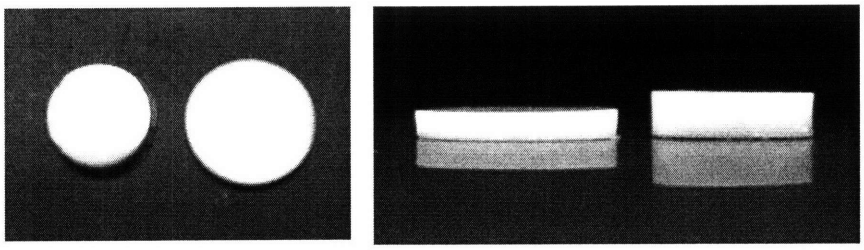

Figure 32: PET C samples before and after compression

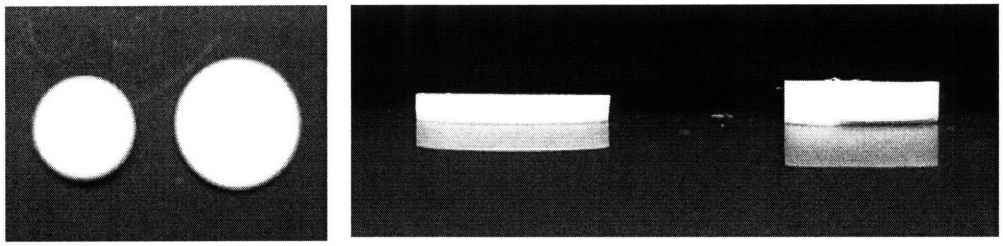

Figure 33: PET B samples before and after compression

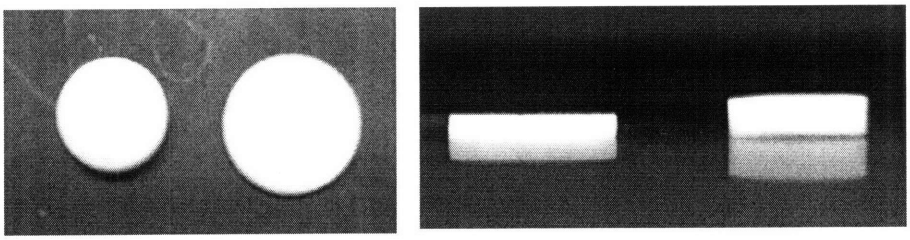

Figure 34: PET A samples before and after compression

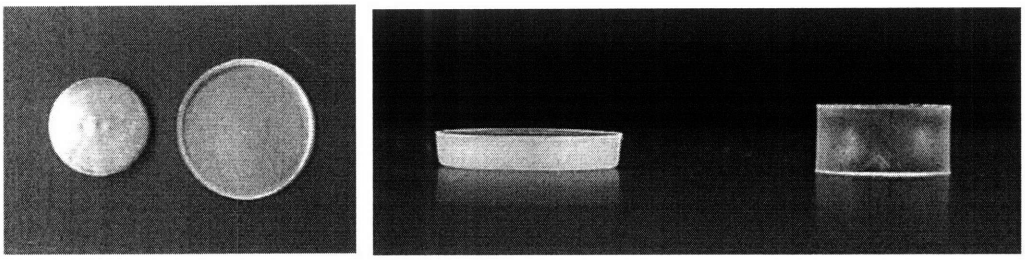

Figure 35: PETG samples before and after compression

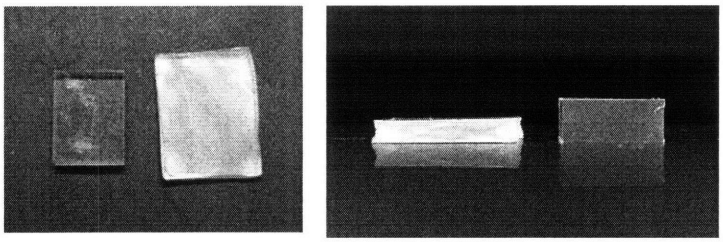

Figure 36: Amorphous PET samples before and after compression

	Strain Rate (1/s)	Test	σ_y (MPa)	E (MPa)
AmPET	0.01	T1	76.2	1646.9
	0.005	T1	74.1	1367.6
	0.001	T2	71.3	1639.7
	0.0005	T1	68.7	1770.6
PETG	0.01	T3	59.5	981.1
	0.005	T2	58.0	1000.8
	0.001	T1	56.7	1073.0
	0.0005	T1	54.0	1134.6
PET A	0.01	5/5 T6	70.4	931.5
	0.005	5/5 T2	67.2	902.8
	0.001	5/5 T1	64.5	944.5
	0.0005	5/5 T1	59.8	813.8
PET B	0.01	T3	89.2	1444.4
	0.005	T3	91.0	1438.6
	0.001	T3	86.9	1545.5
	0.0005	T2	82.0	1304.5
PET C	0.01	T4	92.2	1747.4
	0.005	T3	89.3	1687.6
	0.001	T1	86.3	1439.2
	0.0005	T1	83.5	1370.5
PET D	0.01	T2	91.3	1042.7
	0.005	T3	90.4	1059.2
	0.001	T2	86.8	1057.1
	0.0005	T1	84.9	977.1
PET E	0.01	T2	93.3	1088.7
	0.005	T2	92.2	1075.5
	0.001	T2	87.2	1036.1
	0.0005	T2	83.4	1020.6

Table 3: Yield Stress and Young's Modulus results for each material at each strain rate.